PHILOSOPHICAL TRANSACTIONS OF THE ROYAL SOCIETY A MATHEMATICAL, PHYSICAL & ENGINEERING SCIENCES

Ceramics and Ceramic Composites as High-Temperature Structural Materials: Challenges and Opportunities [and Discussion]

A. G. Evans

Phil. Trans. R. Soc. Lond. A 1995 **351**, 511-527
doi: 10.1098/rsta.1995.0050

Ceramics and ceramic composites as high-temperature structural materials: challenges and opportunities

By A. G. Evans

Division of Applied Sciences, Harvard University, Cambridge, MA 02138, USA and Materials Department, University of Califoria, Santa Barbara, CA 93106, USA

Perspectives are presented on the development of ceramics and ceramic matrix composites (CMCs) for high-temperature structural components. The emphasis is on design requirements and their role in directing research toward actual products. An important theme concerns the relative roles of fracture toughness and inelastic strain (ductility) in the application of materials in primary structures. Ceramics with high toughness have been developed, but macroscopic inelasticity has not been achieved. Robust design procedures have yet to be developed for such materials. This deficiency, as well as relatively high manufacturing and qualification costs, has retarded their commercial exploitation. Strategies for addressing this problem are considered.

CMCs are more 'design friendly' because they exhibit appreciable inelastic strain, in shear and/or in tension. Such strain capacity is an efficient means of redistributing stress and eliminating stress concentrations. The design process thus has commonality with that used for metallic components. Also, processing approaches that provide acceptable manufacturing costs have been devised. The sources of the inelastic strain are examined and models that lead to a constitutive law are described. Some examples are given of its FEM implementation for design calculations.

A limitation on the extensive exploitation of CMCs in high temperature systems has been the existence of degradation mechanisms. These include a 'pest' phenomenon, manifest as oxidation embrittlement in non-oxide CMCs, as well as excessive creep in oxide–oxide CMCs. These degradation mechanisms are discussed, and pathways to affordable high-temperature CMCs are analysed.

1. Introduction

A high-temperature materials research goal for over 20 years has been the creation of structural materials capable of reliable operation, in oxidizing conditions, under tensile stress, at temperatures in the 1200–1400 °C range. This goal has yet to be realized. The strategy has been to begin with materials inherently stable and also deformation resistant at these temperatures, typically ceramics or intermetallics. Components made from such materials are brittle and cannot be used reliably when subject to tensile stress. The addition of reinforcements is

Phil. Trans. R. Soc. Lond. A (1995) **351**, 511–527
Printed in Great Britain

envisaged as the means of introducing damage tolerance without compromising stability and deformation resistance. In practice, various approaches have been found that provide damage tolerance, but the stability and deformation resistance have always been detrimentally affected. Moreover, at least one property of such materials has invariably been found deficient: either toughness or creep strength or embrittlement sensitivity. High manufacturing costs are also problematic in many cases. The consequence is that comparisons with existing metallic systems, on a cost/benefit basis, are not favorable. The result has been a dearth of applications. An alternative research and development strategy is needed if such materials are to be implemented on a large scale in commercial systems. The ingredients include an intelligent processing regimen along with a cost estimation methodology, as well as robust performance models to supplement the manufacturing and design engineering.

The initial goal of the research on monolithic ceramics during the 1960s was to create 'ductile' ceramics by inducing plasticity. This goal did not have a meaningful technological outcome for one principal reason. Even when some ductility was achieved, the materials still had a low fracture toughness and were prone to catastrophic rupture (Clarke *et al.* 1967; Wiederhorn *et al.* 1970). This seeming paradox arose because cracks remained sharp instead of exhibiting plastic blunting. A complete theory describing this phenomenon has yet to be developed, although recent progress has been considerable (Rice & Beltz 1994; Xu *et al.* 1995; Hirsch & Roberts 1991).

The practical consequence of the early work on ceramics was a change in emphasis toward research on *toughening mechanisms*. The effort on 'toughened' ceramics resulted in major discoveries of mechanisms with robust theories capable of characterizing the principal effects. However, the technological ramifications have still been minimal. The lack of a translation of the physics and mechanics to the technology seems to reside in two deficiencies. (1) The high-toughness materials, when tested in tension, are still macroscopically linear. The consequence is that strain concentration sites are also regions of high stress. That is, the material has no mechanism for redistributing stress. The importance of this 'deficiency' has been highlighted as a result of the development of ceramic matrix composites. (2) The implications of the toughening to the design of ceramic components has not been formulated in a manner that can be explicitly used by the design engineer. (Note that the toughness does not appear as a parameter in design codes used for metals, ceramics or composites.)

The development of continuous fibre-reinforced ceramics (ceramic matrix composites (CMCs)) was instituted as a means of obviating the limitations associated with the 'toughened' monolithic materials. Following some crucial discoveries in the 1970s (Phillips 1974; Aveston *et al.* 1971) a large effort was made starting in the 1980s (Prewo 1987; Naslain, this volume). The major finding during this period was that composites can be microstructurally designed to induce inelastic deformation mechanisms in either tension or shear (Evans & Zok 1994). These provide sufficient strain to enable extensive stress redistribution at strain concentration sites, such as slots, joints and attachments (Cady *et al.* 1994; Mackin *et al.* 1995). This capability has allowed a design strategy similar to that used with metals. These advantages have given a stimulus to the continued development of composites. However, there are performance limitations governed by high-temperature degradation mechanisms.

PHILOSOPHICAL TRANSACTIONS OF THE ROYAL SOCIETY A MATHEMATICAL, PHYSICAL & ENGINEERING SCIENCES

2. Technology for design

(*a*) *Monolithic ceramics*

(i) *Stochastic principles*

There have been two complementary philosophies for implementing ceramics (Lange 1989; Evans 1982). One approach has been to elevate the fracture toughness. The other has emphasized a reduction in the size of the flaws introduced by processing and machining. Neither approach has had a profound effect on the technology, despite major scientific and engineering advances in both areas. Designing a load-bearing component using a linear material requires the following steps. (1) An elastic analysis is performed to obtain the stresses. (A problem arises for zones having high localized strain. Then there are mesh effects and sometimes singularities, particularly at joints, attachments and contacts. A design decision must be made about how to address these regions. Some approaches have been recommended, but software has not been made available. While these areas remain problematic, they are not given further consideration.) (2) The survival probability of each element within the finite-element mesh is evaluated using the principles of weakest link statistics (Freudenthal 1967; Matthews *et al.* 1976). The procedure required for this purpose is understood and has been implemented in software programs, CARES (among others), compatible with finite-element codes. The programs calculate the survival probability ϕ_s of volume elements, δV, using

$$\phi_s = 1 - \delta V \int_0^{\bar{\sigma}} g(S)\,\mathrm{d}S, \tag{2.1}$$

where $g(S)\,\mathrm{d}S$ is the number of flaws in unit volume having strength between S and $S + \mathrm{d}S$, and $\bar{\sigma}$ is the average stress within the element at the design load. There is a corresponding formula for the surface elements. The survival probability of the component is the product of the survival probabilities of all of the elements (volume plus surface), $\Pi(\phi_s)$. Usually, $g(S)\,\mathrm{d}S$ is approximated by a power law (Weibull distribution) with a scale parameter, S_0, and a shape parameter, m. When the element size is small (of order the separation between the large extreme of the flaws in the population), this takes the form (Weibull 1939),

$$g(S) = mS^{m-1}/S_0^m. \tag{2.2}$$

The CARES software has the capability of performing these evaluations for any multiaxial state of stress.

The limitation on the practical utilization of the code is in the means for obtaining the data. It is crucial to note that the integration of (2.1) is between zero and the design stress. However, data are normally obtained using flexure tests or tension tests on small specimens. The consequence is that, because of the volume scaling inherent in weakest link statistics (2.1), these tests provide information about the flaw population at stresses above the design stress. An extrapolation of the data is implied (figure 1*a*). A robust procedure for conducting the extrapolation of the available data and for evaluating the confidence limits has not been made accessible to the design engineer. It is usually asserted that the scale and shape parameters obtained from laboratory data apply with high confidence at stresses below the design stress. Such assertions are not valid. Moreover, since (2.2) has no fundamental basis. A polynomial fit to the data could be made

PHILOSOPHICAL TRANSACTIONS OF THE ROYAL SOCIETY A MATHEMATICAL, PHYSICAL & ENGINEERING SCIENCES

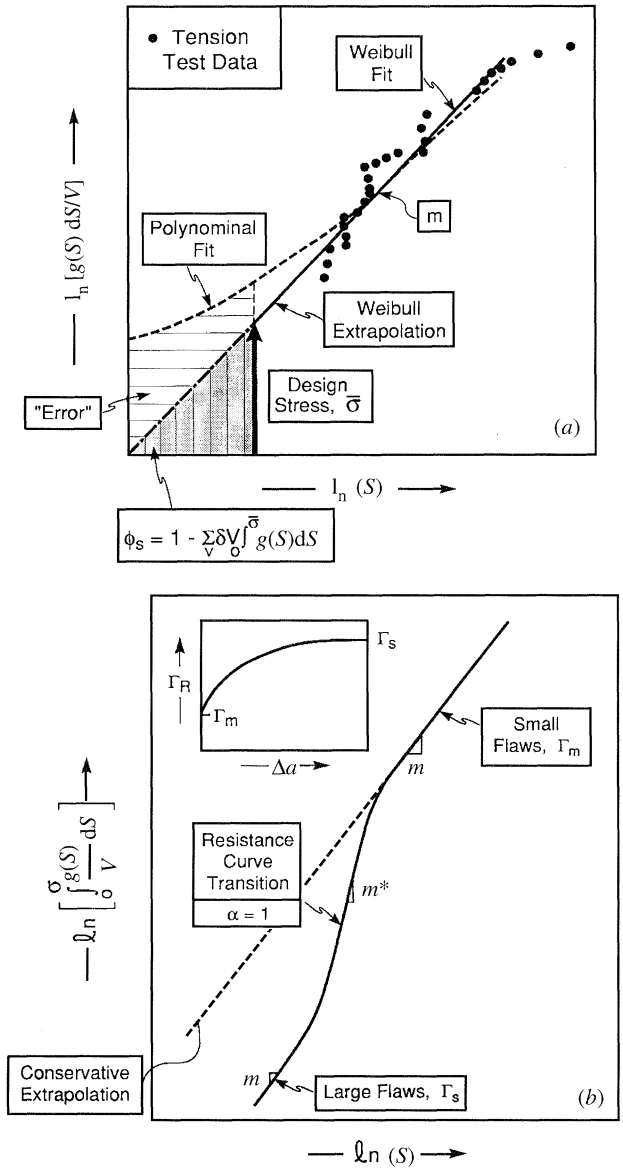

Figure 1. (*a*) Typical statistical data obtained upon tension testing of ceramics. The extrapolation from the (linear) Weibull fit is shown, as well as the extrapolation from a polynomial fit. These indicate the large difference in the projected survival probability (note that the axes are logarithmic). (*b*) Superior confidence associated with extrapolation when a toughened ceramic is used at the optimum value of the strengthening index, α. Note that there is a change in slope from m to m^* when $\alpha \approx 1$. This change enables a larger survival probability for the same flaw population. It is important to appreciate that levels of toughening having smaller values of α do not improve the survival probability.

with equal fidelity, resulting in substantial differences in the predicted survival probability (figure 1*a*).

To obviate this problem and to assure that an acceptable level of confidence is attributed to m and S_0, tests should be performed on relatively large tension specimens to obtain data close to the design stress (figure 1*a*). The gathering of

such data is costly. The costs can probably be justified when the processing and machining have been standardized and subjected to a rigorous control regimen, such that the flaw populations are stable and consistent. In this case, results from proof tests and field tests augment the laboratory data and greatly enhance the confidence levels assigned to the design. Otherwise, batch-to-batch variations and deviations among machining runs result in flaw population changes that have to be recalibrated to provide the level of confidence required for design. The associated costs are usually prohibitive. There is a clear opportunity to implement a processing regimen using a control strategy that regulates the scale and shape parameters that characterize the flaw population.

(ii) *Toughness in design*

An early discovery in the quest for toughening mechanisms was the prevalence of resistance-curve behaviour (McMeeking & Evans 1982; Green *et al.* 1989; Evans 1990; Stump & Budiansky 1988). The main focus of the subsequent research was on the quantification of the resistance through a mechanism-based development of bridging laws and inelastic constitutive laws. However, all of the approaches still resulted in linear stress–strain characteristics upon tensile testing. Since non-linearity was not achieved, the elastic design strategy described above must still be implemented. The toughness itself does not enter the design code. Only its influence on the stochastic strength parameters, m and S_0 is relevant to design (Kendall *et al.* 1986; Cooke & Clarke 1988). This influence can be characterized by a non-dimensional strengthening index, designated α, given by

$$\alpha = (a_0/h_s)(\Delta\Gamma_s/\Gamma_m)^2, \tag{2.3}$$

where a_0 is the initial flaw size, $\Delta\Gamma_s$ is the steady-state toughness elevation, Γ_m the reference toughness in the absence of the toughening mechanism, and h_s is the crack extension needed to reach steady state. This index is a measure of the toughening rate, as the crack extends. Its effect is reflected in the magnitude of the ensuing strength, S, given by

$$\frac{S}{S_*} = \left\{\frac{\alpha\sqrt{(1+\alpha)}}{\alpha + (\sqrt{(1+\alpha)} - 1)^2}\right\}^{1/2}, \tag{2.4}$$

where S_* is the strength at toughness Γ_m, in the absence of toughening.

The key result provided by this analysis is illustrated in figure 1*b*. When the flaws are very small ($\alpha \ll 1$), fracture occurs unstably and the strength is unaffected by the toughening. Conversely, larger flaws are able to experience stable crack growth and the strength may substantially exceed the untoughened magnitude. The transition between the small and large crack regions has particular significance (figure 1*b*). In this region, the effective shape parameter m^* becomes relatively large ($m^* > m$). The consequence is that the survival probabilities, estimated by extrapolation from the small flaw data obtained in typical laboratory tests would be conservative, provided that the processing and machining flaws that dictate the strength near the design stress satisfy, $\alpha \approx 1$. An evident goal for toughening and processing research is to identify and incorporate mechanisms that enable α to be of order unity at the design stress. Such optimization alleviates (but does not solve) the extrapolation problem.

PHILOSOPHICAL TRANSACTIONS OF THE ROYAL SOCIETY A MATHEMATICAL, PHYSICAL & ENGINEERING SCIENCES

(b) Ceramic matrix composites

(i) Stress redistribution

Ceramic matrix composites (CMCs) have two characteristics that greatly facilitate their use as structural materials. (1) Their microstructural design imparts macroscopic inelastic deformation modes. These modes are very efficient at redistributing stress. The important consequence is that stress concentrations are largely eliminated at locations subject to large local strains. Sufficient understanding of the deformation has been gained to enable the development of constitutive laws which have already been implemented in finite-element codes such as ABAQUS (Xia & Hutchinson 1994; Xia *et al.* 1993; Genin & Hutchinson 1995). The calculations demonstrate that the inelastic strain allows the stresses to spread out and have relatively low peak magnitudes.

(2) The design procedure compares the peak stresses to the ultimate strengths, in tension (UTS) and shear, as governed by the *in situ* fibre bundle strength. The stochastic parameters that govern the fibre bundle strength are 'design friendly'. In particular, the shape parameter, m, is quite large (small variability) because the strength is controlled by multiple fibre failures, rather than the weakest link (Curtin 1991). This distribution approaches a Gaussian form (as in metals) and designers use standard deviations to obtain design allowables, enabling a high confidence level to be assigned to the survival probability.

(ii) Inelastic strains

The inelastic deformation of woven or laminated 0/90 CMCs in both tension and shear, occurs in accordance with one of two behaviours, designated class II and class III (Evans & Zok 1994). The former, are 'matrix dominated'. The inelastic strains are largely determined by matrix cracking, with interface debonding and frictional slip. The UTS is dictated by the fibre failure characteristics. In the class III, 'fibre dominated' CMCs, the inelastic tensile strains are controlled by the fibres, whereas the inelastic shear strains are governed by matrix damage. In both types of CMC, stress redistribution is dominated by the inelastic strains arising from matrix damage, particularly those in shear and in ± 45 tension, which occur at the lowest stress levels (figure 2).

(iii) Design calculations

Representative design calculations for CMCs are used to illustrate the importance of stress redistribution mechanisms. Calculations have been performed for tensile plates containing holes or slots. Others have been conducted for pin-loaded holes in order to simulate mechanical attachments made to either superalloy or Ti alloy supports (figure 3). Experimental comparisons obtained using Moire interferometry substantiate the fidelity of the calculations (Cady *et al.* 1994; Mackin *et al.* 1995; Genin & Hutchinson 1995). These measurements give the full strain distribution around the hole.

Both the calculations and Moire measurements illustrate the difference between class II and class III CMCs. For the former, strain concentrations persist. Yet, the stress concentration is small because the inelastic deformation caused by matrix cracking provides an effective means of redistributing stress. Conversely, for class III CMCs, the shear strain localizes into bands, causing both the strain and stress concentrations to be substantially reduced.

PHILOSOPHICAL TRANSACTIONS OF THE ROYAL SOCIETY A MATHEMATICAL, PHYSICAL & ENGINEERING SCIENCES

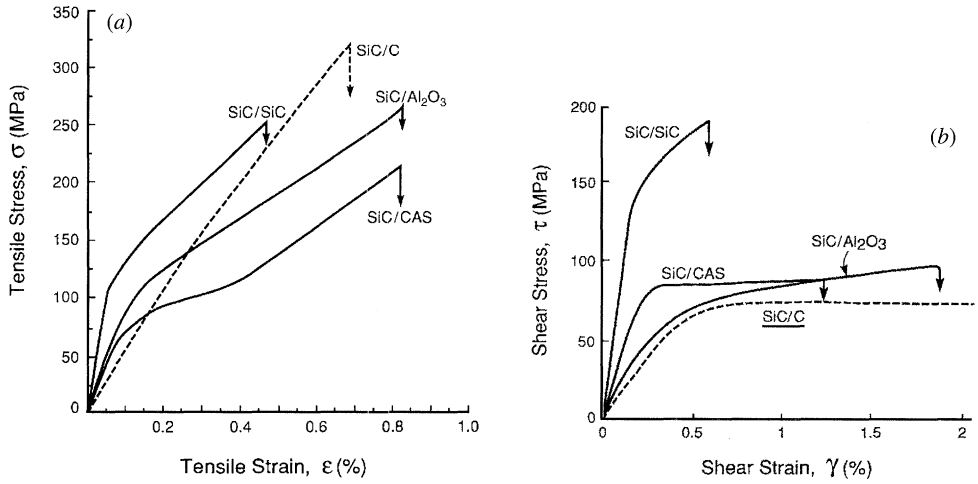

Figure 2. Typical stress–strain curves for CMCs: (*a*) tension; (*b*) shear. The class II CMCs are represented by the solid lines and the class III CMCs by the dotted lines.

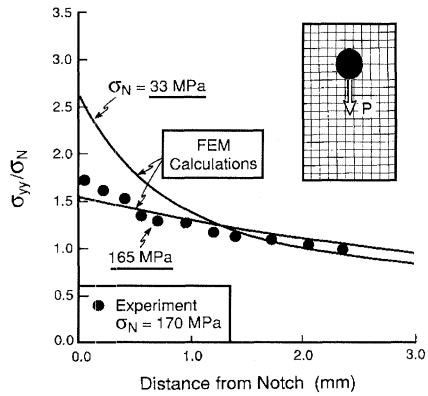

Figure 3. A pin loaded hole test performed on SiC–CAS showing the stress across the net section. The calculated and measured values are indicated. The stresses are obtained from the strains by Moire interferometry. This can be done because the lateral strains are essentially zero.

The stress–strain calculations and measurements are not in complete accordance with other experimental findings for sharp notches. Tension tests reveal notch insensitive strengths, indicative of the material's ability to completely eliminate stress concentrations (figure 4). Such behavior is not predicted by inelastic FEM calculations. The implication is that another stress redistribution mechanism operates in CMCs. It is believed that fibre pull-out is the operative mechanism (figure 4). When fibres begin to fail near the slot, their stochastics dictate a spatial distribution of fibre failure sites. This causes pull-out to occur at the matrix cracks, which reduces the stress on the intact fibres and enables additional load to be imposed before catastrophic failure occurs in the composite (Bao & Suo 1993). A complete simulation capability for design purposes requires that this pull-out effect be included. This implementation is in progress.

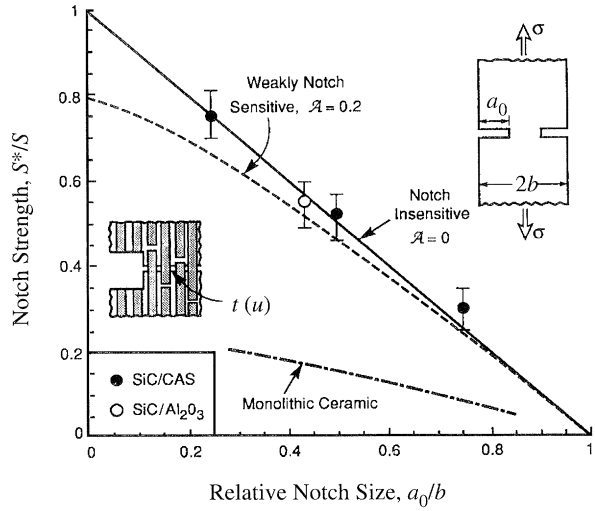

Figure 4. The notch insensitive behaviour found for two class II CMCs. The inset shows the pull-out mechanism. This combines with the inelastic strain mechanism provided by matrix cracking to eliminate the stress concentration at the notch.

3. Inelastic deformation mechanisms

(a) *Basic concepts*

Brittle matrix composites exhibit inelastic deformations when microcracks are stabilized. This is achieved by using either fibre coatings or porous matrices to deviate cracks toward the loading axis (figure 5), in accordance with the concept originally proposed by Cook & Gordon (1968). The resultant composite microstructure and the ensuing mechanical responses (Tu *et al.* 1995) resemble those found in various naturally occurring materials, such as wood. The fundamental requirement is that the crack deviating sites be homogeneously dispersed and have a low shear debond energy Γ_i relative to the fracture energy Γ_s of the fibre bundles. The most stringent stabilization requirement arises when there are no residual stresses. It is given by (He & Hutchinson 1989)

$$\Gamma_i < \tfrac{1}{4}\Gamma_s. \tag{3.1}$$

Residual compression in the deviation zone facilitates crack stabilization (figure 5). Once the deviation criterion has been satisfied, the extent of the inelastic strain is governed primarily by the number density of deviation sites and the friction stress that operates along the debonded surfaces. Two cases have been considered. (1) Composites that use a fibre coating to deviate the cracks – designated CMC-Cs. (2) Composites that use a porous matrix for crack deviation purposes – designated CMC-Ms (figure 5).

The inelastic strain of woven or laminated 0/90 CMCs increases and the flow stress decreases as the principal stresses deviate from the fibre axis (Cady *et al.* 1995). The lowest strains and the largest stresses obtain for 0/90 tensile loading. The largest strains and smallest stresses occur for shear loading: although off-axis tensile loading between 30 and 45° induces similar large strains. Fibre failure only contributes to the inelastic strains upon 0/90 tensile loading.

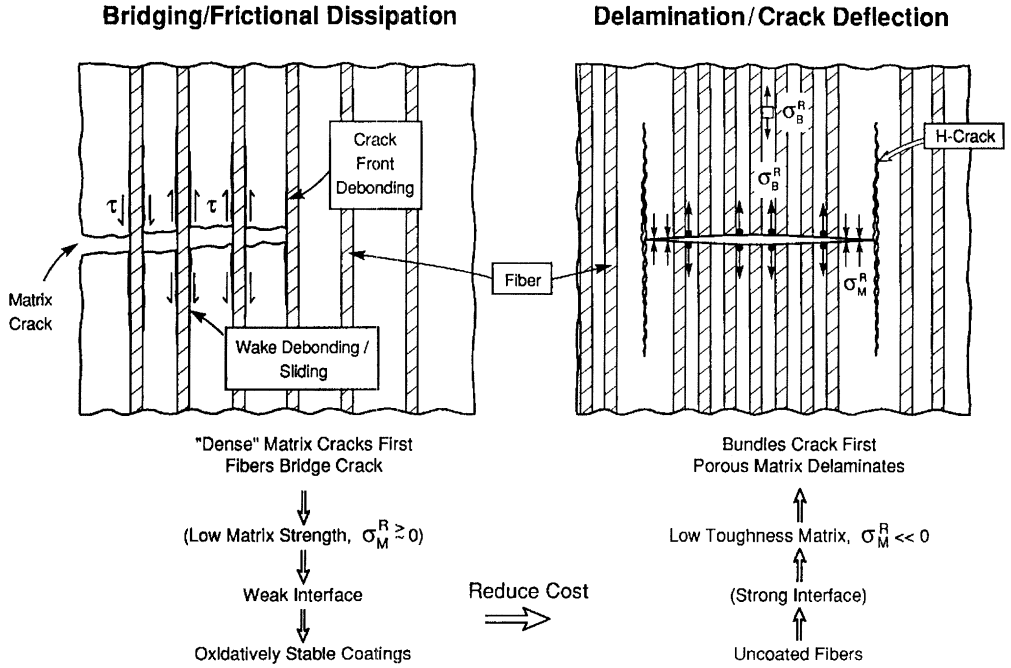

Figure 5. The two concepts for deviating cracks and inducing frictional dissipation along the debonded surfaces. (*a*) The use of a fibre coating to give an interphase capable of debonding, followed by friction. (*b*) A porous matrix, combined with residual compression, that causes debonding by H-cracking, with subsequent friction.

(*b*) *Debonding and friction*

Shear debonding is commonly encountered in thin brittle layers. It comprises the formation and eventual coalescence of microcracks *en echelon* within a cohesive zone. The associated fracture energy is (Xia *et al.* 1994) $\Gamma_i \approx 4\Gamma_0$, where Γ_0 is the mode I fracture toughness of the material in the layer. Recall that for debonding, inequality (3.1) must be satisfied, (3.5). This very stringent requirement eliminates all but a few debond concepts (Davis *et al.* 1993; Kerans 1994). The microcracks behind the debond coalescence and fragment the layer. This process induces friction at contacting asperities, resulting in a slip zone subject to a friction stress, τ. This stress is found to have essentially constant magnitude within the slip zone, although it varies among the different CMCs, from about 2 MPa in SiC–LAS to about 100 MPa in SiC–SiC (Evans & Zok 1994). It also diminishes upon cyclic loading and increases upon oxidation.

Qualitative models indicate that τ is affected primarily by the roughness amplitude behind the debond (Parthasarathy *et al.* 1994). The residual stress, the elastic compliance of the circumventing material and the friction coefficient may also be important. Present understanding is sufficient to allow τ to be systematically varied when fibre coatings are used. This is achieved by adjusting the coating thickness, its porosity and the matrix compliance.

(*c*) *Stochastic fibre failure*

In CMCs having fibre coatings, the stochastics of fibre failure are well established (Curtin 1991). When the debond and friction stresses are both relatively

low, the stress concentration that would otherwise develop in the circumventing material is eliminated. This feature enables fibre failures to occur in a spatially uncorrelated manner, resulting in global load sharing (GLS) characteristics. In such cases, friction allows stress transfer between the fibre and the matrix. The consequence is that, beyond a slip length l, the stress in the fibre is unaffected by the existence of the failure and l dictates the gauge length governing the fibre bundle strength. The ultimate tensile strength is given by

$$S_{\mathrm{u}} = fS_{\mathrm{c}}F(m), \tag{3.2}$$

where f is the fibre volume fraction, S_{c} is the characteristic strength and $F(m) \approx 0.7$. The fibre failures also produce a small inelastic strain upon loading along the fibre axis. This strain has some importance in class III CMCs.

Stress concentrations in the fibres caused by unbridged matrix cracks may reduce the UTS below the GLS level. The extent of such stress concentrations is governed by a stress concentration index, η, in accordance with the relation (Budiansky & Cui 1994; Xia *et al.* 1994),

$$S/S_{\mathrm{u}} = \sqrt{[1 + (\eta\beta)^{2/3}]}, \tag{3.3}$$

with

$$\eta = \frac{3\pi f^2 E_{\mathrm{f}} E^2 a\tau}{(1-f)^2 E_{\mathrm{m}}^2 \bar{E} RSA},$$

where a is the size of the largest unbridged crack or manufacturing flaw, f is again the fibre volume fraction and A is an anisotropy coefficient. The quantity β, which depends on f, and $E_{\mathrm{f}}/E_{\mathrm{m}}$ is a large-scale slip coefficient. For typical f and $E_{\mathrm{f}}/E_{\mathrm{m}}$, $\beta \approx \frac{1}{3}$. In 0/90 CMCs, a is typically the ply dimension, h, although manufacturing flaws could cause a to exceed h in severe cases. Note that η must exceed unity before there is a significant reduction in the UTS below the GLS value. Imposing this condition yields a maximum acceptable τ that ensures the GLS strength, $\tau_{\max} \approx 50$ MPa. Otherwise the strength will be lower than the GLS magnitude and the material would have a diminished inelastic tensile strain capacity.

(*d*) *Matrix cracking*

An understanding of the important role of matrix cracking has been gained from studies performed on 0/90 composites having fibre coatings that control debonding and friction. These have mostly been class II CMCs that exhibit considerable inelastic strain in both tension and shear. However, the resulting methodology appears to be more general, though phenomenological.

Two-cell models represent most of the features found upon loading class II CMC-Cs in the 0/90 orientation (Xia *et al.* 1994; Hutchinson & Jensen 1990). One model is for cracks that first form in the 90° plies (figure 6*a*). The other represents cracks that penetrate the 0° plies (figure 6*b*). Cracks in either woven or laminated 0/90 CMCs form first in the 90° plies by tunnelling at a critical strain ϵ_{t}, given by

$$\epsilon_{\mathrm{t}} E_{\mathrm{T}} = g\sqrt{(E\Gamma_{\mathrm{m}}/h)} - \sigma_{\mathrm{R}}, \tag{3.4}$$

where Γ_{m} is the matrix fracture energy, σ_{R} is the ply level residual stress, E is the composite Young's modulus, E_{T} is the transverse Young's modulus, h is the ply thickness and g is a coefficient of order unity that depends on the transverse

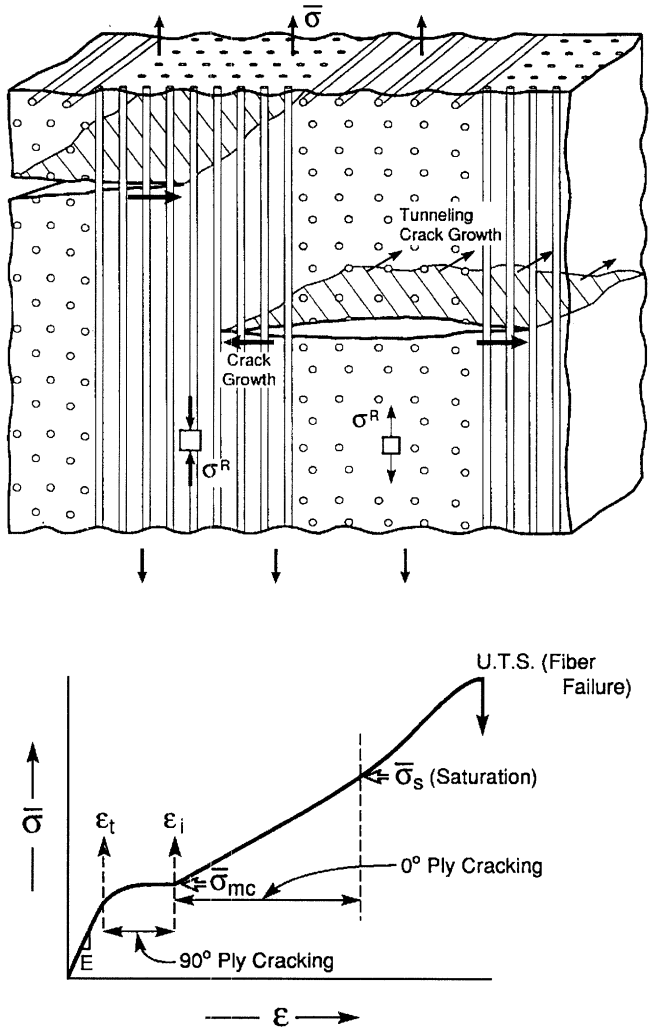

Figure 6. (*a*) The ply cracking model for a 0/90 CMC tested in tension. The associated stress–strain curve indicates the inelastic strains from sequential matrix cracking of the 90° and 0° plies, with the fibres intact.

attachment between the fibres and the matrix. At strains just above this critical condition there is a rapid change in the inelastic strain (figure 6*a*).

Upon subsequent loading, as the cracks penetrate the 0° plies, they interact with the fibres and the coating. When debonding and slip occur within the coating, the inelastic strain may be characterized by two stresses: a friction stress τ, and a debond stress σ_i. The latter is related to the debond toughness for the coating (Hutchinson & Jensen 1990; Budiansky *et al.* 1995). The strain ϵ depends on the stress σ acting on the 0° plies, in accordance with (Domergue *et al.* 1995)

$$\epsilon = 2L\sigma^2(1-\Sigma_i)(1+\Sigma_i+2\Sigma^T) + (1+\Sigma^T)\sigma/E_* - \sigma^T/E, \qquad (3.5)$$

where Σ_i is the non-dimensional debond stress, $\Sigma_i = \sigma_i/\sigma$, E_* is the diminished elastic modulus caused by matrix cracking and L is an interface friction index,

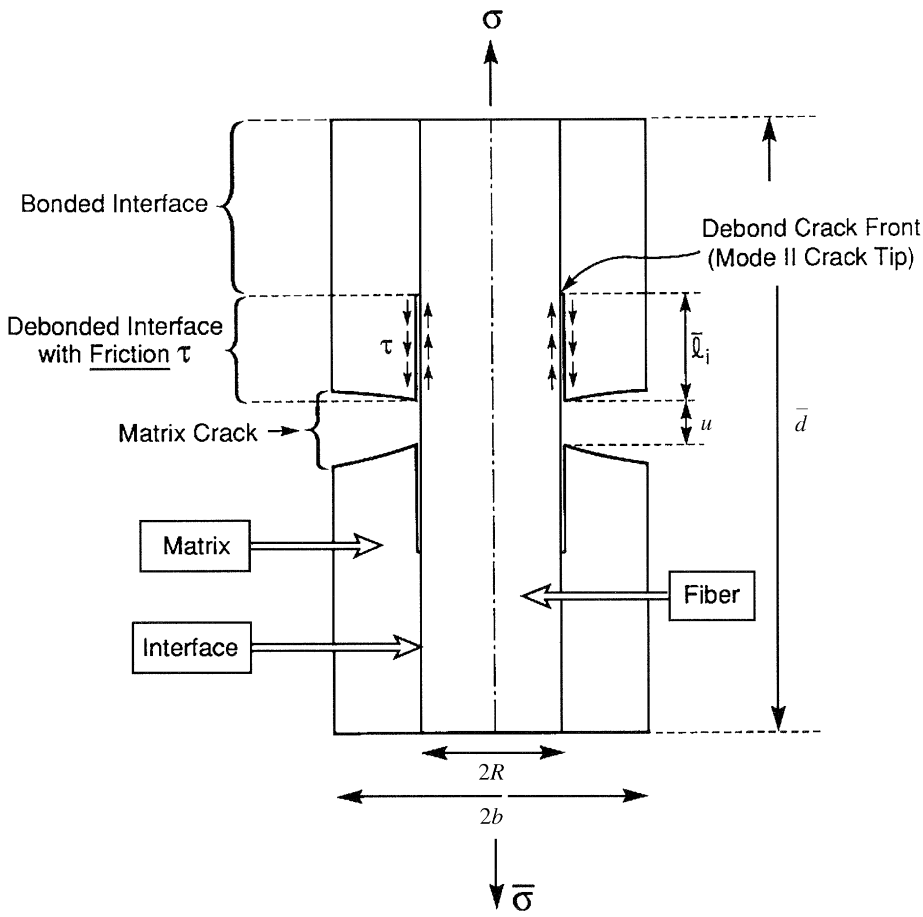

Figure 6. (*b*) The cell model for cracking of the 0° plies. The interface responses are characterized by a debond energy and a friction stress. These determine the inelastic strain in the presence of a matrix crack.

given by

$$L = \frac{b_2(1 - a_1 f)^2 R}{4 f^2 \tau d E_m}$$

with d being the crack spacing and the coefficients a_1 and b_2 are of order unity (defined in the paper by Hutchinson & Jensen (1990)). Note that the influence of friction on the strain appears as a product, τd, of the friction stress and the crack spacing. Separate determination of τ is not required for simulation of the strains.

It has been demonstrated that E_*, L and Σ_i can be evaluated by using hysteresis strain measurements, upon plotting the tangent compliance as a function of stress (Pryce & Smith 1993; Domergue *et al.* 1995; Cady *et al.* 1995). L is obtained from the slope, E_* from the intercept and Σ_i from the slip–no-slip transition stress. With these parameters determined, σ^T can be evaluated from the remanent strain. The parameters obtained directly from the hysteresis measurements enable

the strains to be simulated. Such simulations have two roles. (1) They afford a consistency check on the methodology.

(2) They provide understanding about the separate influences on the strain provided by debonding, friction and matrix cracking.

4. Degradation by oxidation embrittlement

All non-oxide CMCs are susceptible to a 'pest' phenomenon that operates at intermediate temperatures, between 500 and 900 °C (figure 7). The degradation happens most readily at strain concentration sites, where matrix cracks have been created upon loading. These matrix cracks become pathways for the relatively rapid ingress of oxygen into the material (Brennan 1986; Heredia *et al.* 1995; Naslain, this volume). When the fibres and the coatings are non-oxides, the oxygen reacts to form both solid and gaseous products (Raj 1993). There are two consequences. (1) The fibres are weakened, because of flaws and residual stresses induced by the solid reaction product. (2) The friction stress changes and increases the stress concentration on the fibres at the perimeter of the cracks in the 90° plies (equation (3.3)). The degradation in the fibre strength combines with the increase in stress concentration to embrittle the composite. Typically, the embrittlement commences at the external surface and progressively extends inward, manifest as a region exhibiting negligible fibre pull-out. When the embrittled region has progressed to a sufficient extent, the remaining composite is unable to sustain the load.

Three approaches are being used to address this debilitating problem: (1) an all oxide composite, (2) multiple fibre coatings, and (3) kinetic retardation through coating and fibre chemistry selection.

(*a*) *Oxide composites*

Three different oxide CMCs have been devised. Two are fibre-coated CMC-Cs that use either a fugitive carbon coating (Davis *et al.* 1994) or a low toughness $LaPO_4$ coating (Morgan *et al.* 1994). The carbon coating protects the fibre upon matrix infiltration and may then be eliminated to form a gap. The gap is chosen to be small enough to allow asperity contact between the fibres and matrix to provide the requisite friction, which then controls the inelastic strains. Such CMCs gradually degrade at high homologous temperatures because the matrix sinters to the fibres and introduces flaws that cause weakening.

The third is a CMC-M concept (figure 5) that relies upon a porous matrix to deviate cracks (facilitated by residual compression). A fibre coating is not required (Tu *et al.* 1995). Such composites, exemplified by alumina–mullite, exhibit class III deformation characteristics. That is, stress redistribution is provided by the inelastic shear strain, enabled by two key requirements. (1) The matrix infiltration and heat treatment are performed at a sufficiently low temperature to ensure that fibre degradation is suppressed. (2) The porosity of the matrix and the residual stress are controlled at levels that satisfy debonding requirements.

A present performance limitation arises because all commercial oxide fibres are based on alumina. Such fibres have relatively low creep strength at temperatures above about 1000 °C. Moreover, these polycrystalline oxides have low thermal conductivities, leading to poor heat dissipation from regions subject to high heat flux. This induces high temperatures in the CMC causing an exacerbation of the

PHILOSOPHICAL TRANSACTIONS OF THE ROYAL SOCIETY A MATHEMATICAL, PHYSICAL & ENGINEERING SCIENCES

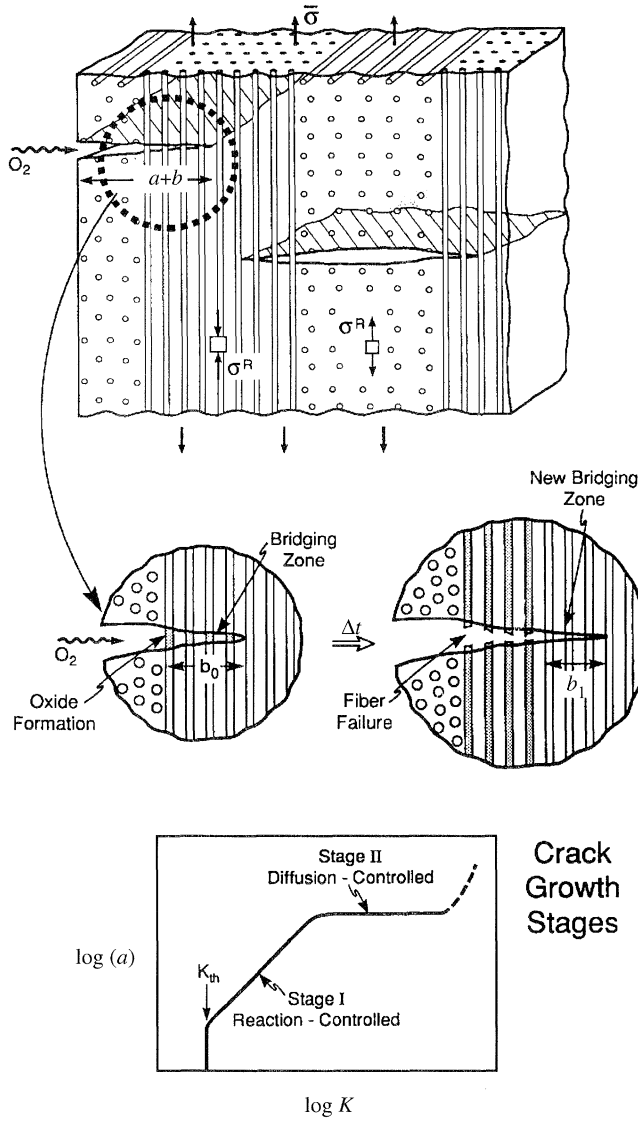

Figure 7. The phenomena that occur during oxidation embrittlement. The top view illustrates that O_2 diffuses through the matrix cracks and reacts with the exposed non-oxide fibres in the bridging zone, within the 0° plies, to form an oxide. This oxide layer weakens the fibres and causes them to fail. The crack then extends and the process repeats. The phenomenon is similar to high temperature stress corrosion cracking. It can be characterized in the same manner, shown on the bottom, through reaction and diffusion controlled regimes of crack propagation, dependent on the stress intensity factor, K.

fibre creep problem. Because of these limitations, the development of creep resistant oxide fibres continues.

(*b*) *Multiple coatings*

Multiple coating concepts have been suggested that have the potential for eliminating embrittlement in non-oxide CMCs (Kerans 1995; Naslain, this volume). One such concept proposes a triple coating. Two of the coatings would be comprised of

mullite, which is chemically compatible with SiC. The third, located between the other two, is a fugitive C coating. In principle, the thickness of this coating could be chosen to control the friction stress, but the concept has yet to be tried. A SiC–SiC composite with such a coating system should exhibit attractive thermal properties.

(*c*) *Kinetic retardation*

By understanding the embrittlement mechanism, its kinetics could be specified and lifetime predictions used to evaluate the acceptability of each CMC for specific applications. The phenomena that govern the embrittlement are illustrated on figure 7. Oxygen from the environment migrates into the narrow matrix cracks. Some of the oxygen diffuses into the fibres and forms an oxide reaction product. This reaction consumes some of the incoming oxygen. The consequence is a time evolution of the oxygen concentration in the cracks. When the oxide reaches a critical thickness, all of the exposed fibres within the crack fail and the crack extends by an amount equal to the fibre bridging zone size. A new bridging zone of pristine fibres is then exposed and the process repeats. Analysis of this phenomenom (Evans *et al.* 1995) has indicated a power law dependence of the failure time on the applied stress. However, the major material factor affecting the embrittlement kinetics is the diffusivity in the oxide, D_0. This is dramatically influenced by purity, especially if it is silica-based. Small amounts of B and alkalies (Ca, Mg, etc.), profoundly increase D_0. High-purity fibres thus provide an opportunity to retard embrittlement and enhance the life expectancy of non-oxide CMCs.

5. Opportunities

Ceramics have the disadvantage that weakest link statistics must be used for design. It is crucially important that the survival probabilities associated with design stress levels be specified with high confidence. In turn, this requires an intelligent processing regimen, using a control model that regulates the stochastic strength. Applying such a regimen has particular advantages when a toughened ceramic is used, because of the diminished variability and the greater confidence associated with data extrapolation.

The research challenges for CMCs are quite different. Their inelastic deformation enables the application of 'Gaussian' statistics, enabling the implementation of familiar design rules used for metal and polymer composites. The problems concern high temperature degradation. For non-oxide CMCs, oxidation embrittlement is the most debilitating. Retarding the degradation requires research on multiple coating concepts as well as on the development of fibres having high purity and acceptable manufacturing costs. High-purity SiC fibres appear to be the only realistic material. However, embrittlement would still be life limiting and its kinetics ultimately govern the applications.

Oxide–oxide CMCs present different challenges. In these materials, fibre creep limits performance. Affordable single crystal fibre growth is impractical. Among the affordable polycrystalline oxides, mullite is the material of choice. However, greater understanding is needed to project the behaviour of oxide fibres having high creep strength.

PHILOSOPHICAL TRANSACTIONS OF THE ROYAL SOCIETY A MATHEMATICAL, PHYSICAL & ENGINEERING SCIENCES

References

Aveston, J., Cooper, G. A. & Kelly, A. 1971 Single and multiple fracture. In *Properties of Fiber Composites: Conf. Proc. National Physical Laboratories*, pp. 15–26. Surrey, UK: IPC Science and Technology Press.

Bao, G. & Suo, Z. 1992 *Appl. Mech. Rev.* **45**, 355–66.

Brennan, J. J. 1986 *Tailing of multiphase ceramics* (ed. R. Tressler), p. 549. New York: Plenum.

Becher, P. F. & Tiegs, T. N. 1987 *Am. Ceram. Soc.* **70**, 651–654.

Budiansky, B. & Cui, L. 1994 *J. Mech. Phys. Solids* **42**, 1–19

Budiansky, B., Evans, A. G. & Hutchinson, J. W. 1995 *Int. J. Solids Struct.* **32**, 315–328.

Cady, C., Heredia, F. E. & Evans, A. G. 1995 *J. Am. Ceram. Soc.* (In the press.)

Cady, C., Mackin, T. E. & Evans, A. G. 1995 *J. Am. Ceram. Soc.* **78**, 77–82.

Clarke, F. J. P., Sambell, R. A. J. & Tattersall, H. G. 1962 *Phil. Mag.* **7**, 393–413.

Cooke, R. F. & Clarke, D. R. 1988 *Acta metall.* **36**, 555.

Curtin, W. 1991 *J. Am. Ceram. Soc.* **74**, 2837.

Davis, J. B., Lofvander, J. P. A. & Evans, A. G. 1993 *J. Am. Ceram. Soc.* **76**, 1249–1257.

Domergue, J.-M., Vagaggini, E., Evans, A. G. & Parenteau, J. 1995 *J. Am. Ceram. Soc.* (In the press.)

Evans, A. G. 1982 *J. Am. Ceram. Soc.* **65**, 127–137.

Evans, A. G. 1990 *J. Am. Ceram. Soc.* **73**, 187–206.

Evans, A. G. & Zok, F. W. 1994 *J. Mater. Sci.* **29**, 3857–3896.

Evans, A. G., Zok, F. W. & McMeeking, R. M. 1995 *Acta metall. Mater.* (In the press.)

Freudenthal, A. 1967 *Fracture* (ed. H. Liebowitz), pp. 341–345. New York: Academic Press.

Genin, G. & Hutchinson, J. W. 1995 *J. Am. Ceram. Soc.* (In the press.)

Gordon, J. E. 1968 *The new science of strong materials*. London: Penguin.

Green, D. J., Hanninck, R. H. & Swain, M. V. 1989 *Transformation toughening of ceramics*. Boca Raton, FL: CRC Press.

He, M. Y. & Hutchinson, J. W. 1989 *Int. J. Solids Struct.* **25**, 1053–1067.

Hirsch, P. B. & Roberts, S. G. 1991 *Phil. Mag.* A **64**, 55.

Hutchinson, J. W. & Jensen, H. 1990 *Mech. Mater.* **9**, 139.

Kendall, K., McNalford, N., Tan, S. R. & Birchall, J. D. 1986 *J. Mater. Sci.* **1**, 120.

Kerans, R. 1994 *Scr. metall. Mater.* **31**, 1075.

Lange, F. F. 1989 *J. Am. Ceram. Soc.* **72**, 1.

Mackin, T. J., Perry Jr, K. E., Epstein, J. S., Cady, C. M., He, M. Y. & Evans, A. G. 1995 *J. Am. Ceram. Soc.* (In the press.)

McMeeking, R. M. & Evans, A. G. 1982 *J. Am. Ceram. Soc.* **65**, 242–247.

Matthews, J. R., Shack, W. J. & McClintock, F. A. 1976 *J. Am. Ceram. Soc.* **59**, 304.

Morgan, P. E. D. & Marshall, D. B. 1995 *J. Am. Ceram. Soc.* (In the press.)

Parthasarathy, J. A., Marshall, D. B. & Kerans, R. 1994 *Acta metall. Mater.* **42**, 3773–3784.

Prewo, K. M. 1987 *J. Mater. Sci.* **22**, 2595.

Pryce, A. W. & Smith, P. A. 1993 *Acta metall. Mater.* **41**, 1269.

Phillips, D. C. 1974 *J. Mater. Sci.* **9**, 1874.

Raj, R. 1993 *J. Am. Ceram. Soc.* **76**, 2147.

Rice, J. R. & Beltz, G. E. 1994 *J. Mech. Phys. Solids* **42**, 333.

Stump, D. M. & Budiansky, B. 1988 *Int. J. Solid Struct.* **25**, 635.

Tu, W., Lange, F. F. & Evans, A. G. 1995 *J. Am. Ceram. Soc.* (In the press.)

Wiederhorn, S. M., Moses, R. L. & Bean, B. L. 1970 *J. Am. Ceram. Soc.* **53**, 18–23.

Weibull, W. 1939 *Ingeniorsvetenskapakademiens* (Handlingar Nr:), p. 153.

PHILOSOPHICAL TRANSACTIONS OF THE ROYAL SOCIETY A MATHEMATICAL, PHYSICAL & ENGINEERING SCIENCES

Xia, C. & Hutchinson, J. W. 1994 *Acta metall. Mater.* **42**, 1935–1945.

Xia, C., Carr, R. R. & Hutchinson, J. W. 1993 *Acta metall. Mater.* **41**, 2365.

Xia, C., Hutchinson, J. W., Budiansky, B. & Evans, A. G. 1994 *J. Mech. Phys. Solids* **42**, 1139–1158.

Xu, G., Argon, A. S. & Ortiz, M. 1995 *Phil. Mag.* (In the press.)

Discussion

J. Rödel (*GDP, Darmstadt, Germany*). Is really large-scale ductility – in the sense of an irreversible displacement in the stress–strain curve – needed, or just a local ductility to mitigate damage in a local scale, by, say, an incoming particle?

A. G. Evans. If you think of large structural components with holes the size of millimetres, large-scale ductility is needed, but not a lot. Ductility less than 1% is sufficient.

PHILOSOPHICAL TRANSACTIONS OF THE ROYAL SOCIETY A MATHEMATICAL, PHYSICAL & ENGINEERING SCIENCES